Regional Differences in Cortical Bone Organization and Microdamage Prevalence in Rocky Mountain Mule Deer

JOHN G. SKEDROS,* CHRISTIAN L. SYBROWSKY, TODD R. PARRY, AND ROY D. BLOEBAUM

Bone and Joint Research Laboratory, Department of Veterans Affairs Medical Center, Salt Lake City, Utah

ABSTRACT

The limb bones of cursorial mammals may exhibit regional structural/material variations for local mechanical requirements. For example, it has been hypothesized that mineral content (%ash) and secondary osteon population density (OPD) progressively change from proximal (e.g., humerus) to distal (e.g., phalanx), in accordance with corresponding progressive changes in stress and mechanical/metabolic cost of functional use (both greatest in the distal limb). We tested this hypothesis in wild-shot Rocky Mountain mule deer by examining transverse segments from mid-diaphyses of medial proximal phalanges, principal metacarpals, radii, and humeri, as well as the lateral aspects of sixth ribs from each of 11 mature males. Quantified structural parameters included the section modulus (Z), polar moment of inertia (J), cortical area/total area ratio (CA/TA), bone girth, and cortical thickness. In addition, %ash and the prevalence of in vivo microcracks were measured in each bone. Thin sections from seven animals were further examined for OPD and population densities of new remodeling events (NREs). Results showed a significant progressive decrease in %ash from the humerus (75.4% ± 0.9%) to the phalanx (69.4% ± 1.1%) ($P < 0.0001$), with general proximal-to-distal increases in OPD and general decreases in J and Z. Thirteen microcracks were identified in the rib sections, and only two were observed in the limb bones. Although the ribs had considerably greater NREs, no significant differences in NREs were found between the limb bones, indicating that they had similar remodeling rates. Equivalent microcrack prevalence, but nonequivalent structural/material organization, suggests that there are regional adaptations that minimize microcrack production in locations with differences in loading conditions. The progressive proximal-to-distal decrease in %ash (up to 6%); moderate-to-high correlations between OPD, %ash, J, and CA/TA; and additional moderate-to-high correlations of these parameters with each bone's radius of gyration support the possibility that these variations are adaptations for regional loading conditions. Anat Rec Part A 274A:837–850, 2003.

Key words: bone adaptation; microdamage; bone mineral content; osteons; mule deer skeleton

It has been postulated that the habitual strain environments experienced by different limb bones in a cursorial animal require regionally specific structural and material adaptations to ensure adequate fracture resistance in each skeletal location (Currey, 1981). As the limb swings through the gait sequence, the distal end must be accelerated and decelerated through a greater range of velocity than that required by the more proximal parts. Some investigators have therefore suggested that reducing distal limb mass would be advantageous in terms of energy conservation (Steudel, 1990a, b; Walker and Liem, 1994; Alexander, 1998).While it would be advantageous for a limb to conserve mass distally in addition to being suffi-

Grant sponsor: Department of Veterans Affairs, Salt Lake City Health Care System; Grant sponsor: Department of Orthopaedics, University of Utah School of Medicine.

*Correspondence to: John G. Skedros, M.D., 5323 Woodrow Street, Suite 202, Salt Lake City, UT 84107. Fax: (801) 983-4903. E-mail: jskedros@utahboneandjoint.com

Received 31 March 2003; Accepted 13 June 2003

DOI 10.1002/ar.a.10102

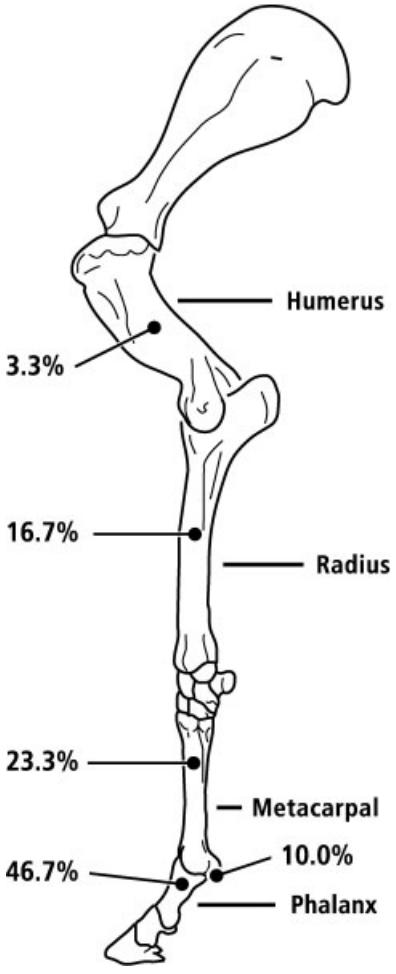

Fig. 1. Horse forelimb showing relative fracture incidence in racing animals that had not fallen, in accordance with data from Vaughan and Mason (1975).

ciently elongated for adequate stride length, the distal elements of a cursorial species are likely to experience greater impact stress and/or energy absorption than the more proximal components. A distal limb bone, therefore, must achieve these objectives while providing superior resistance to the potentially deleterious effects of increased strain and impact stress.

In Currey's (1981) account of a study by Vaughan and Mason (1975), he hypothesized that racehorses are more prone to distal fractures, since these bones are nearer to the point of hoof impact, and thus sustain excessive cyclic loads and endure the greatest stress (Fig. 1). Distal bones would therefore be more susceptible to the accumulation of fatigue microdamage, since lower safety factors might be expected in these regions (Alexander, 1998). Currey hypothesized that different bones in the appendicular skeletons of these animals might exhibit different material adaptations in order to enhance fatigue life in accordance with their different loading conditions. Based on experimental data available at that time showing that remodeled bone is weaker and less fatigue-resistant than primary bone (Currey, 1959, 1975, 1984a; Reilly and Burstein, 1974; Carter and Hayes, 1976; Carter et al., 1976; Wright and Hayes, 1976), Currey suggested that more extensive remodeling (i.e., a greater number of secondary osteons), if required for systemic calcium demands, would be expected to occur in ribs or other relatively non-weight-bearing parts of the skeleton, since these regions can afford the biologic cost of the consequent alteration in safety factor (i.e., the compromised strength resulting from relatively highly remodeled bone). Hence, the least amount of remodeled cortex (i.e., least amount of secondary osteonal bone) would be found in bones nearest the hoof, and the relative amount of remodeled cortex would increase proximally. In theory, the highly remodeled proximal bones would also have lower mineralization than the bones nearer the hoof, since the formation and presence of secondary osteons typically produces tissue with both higher porosity and lower mineral content (i.e., lower mean tissue age) (Currey, 1984a; Martin and Burr, 1989).

A logical extension of this argument is that in other cursorial animals, an increase in the incidence of fatigue microdamage would occur in the more distal limb bones if regional adaptation were not present. Currey (1981) found a rough approximation of this pattern of remodeled cortical bone in one skeleton of a 3-year-old cat; however, the bones were not examined for mineral content, possible structural adaptations, or in vivo microdamage.

An alternative hypothesis is that more extensively remodeled cortices would be found in the distal bones, with the amount of remodeled bone progressively decreasing toward the axial skeleton. In this scenario, distal bones would exhibit a greater proportion of microdamage-mediated repair than proximal bones, since the more precarious loading environment of distal bones would be more conducive to microcrack formation. An adaptive role for highly remodeled bone has been supported by recent studies showing that osteons may extend fatigue life and increase fracture toughness through various means, which had not been considered or recognized when Currey first examined this issue (Martin and Burr, 1989; Yeni et al., 1997; Jepsen et al., 1999; Brown et al., 2000; Skedros et al., 2001a). Although the relative amount of cortical remodeling representing microdamage repair is unknown, some investigators have suggested that not only is it a large percentage of the total remodeling that occurs during skeletal ontogeny (Martin, 2002), but the resulting remodeled cortex may also attenuate the spread (not the formation frequency) of subsequent microcracks (Reilly et al., 1997; Martin et al., 1998). If this view is correct, the skeleton of mature animals would have a pattern of remodeled cortical bone and mineralization that would be opposite to the pattern suggested by Currey.

Based on these more recent data, we hypothesized that the appendicular skeleton of a large, wild, skeletally mature, cursorial mammal would exhibit a progressive increase in remodeled bone in a proximal-to-distal pattern, opposite that predicted by previous hypotheses (Fig. 2). This implies that relatively equivalent microcrack densities would be found between different limb bones of a mature animal, since, in maturity, regional adaptations that enhance fatigue life should minimize potential regional disparities in microcrack formation. We tested these hypotheses by examining the ribs and bones of the forelimb appendicular skeleton of a sample of wild, mature Rocky Mountain mule deer for the prevalence of in vivo microcracks, bone microstructure, mineral content,

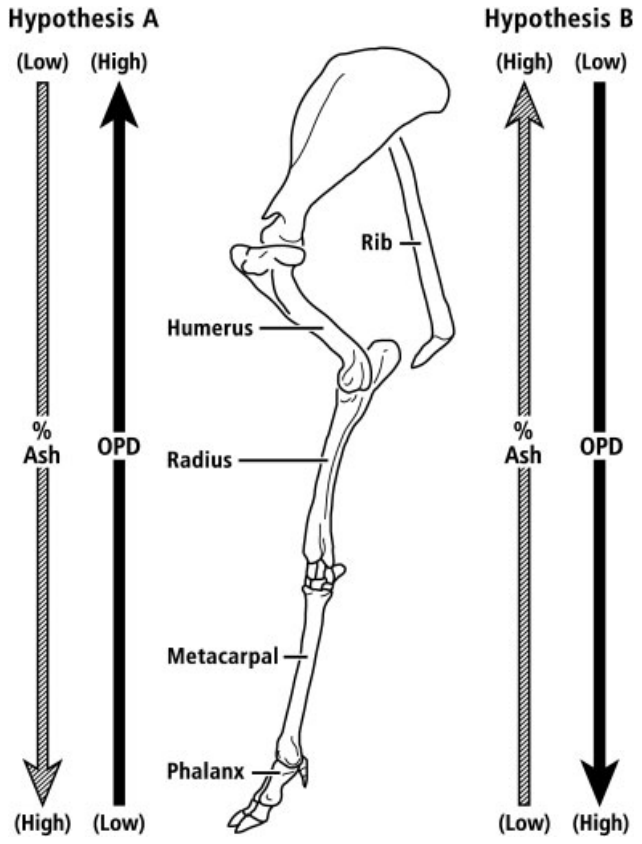

Fig. 2. Deer forelimb, illustrating a previous hypothesis (hypothesis A), such as that proposed by Currey (1981), vs. the hypothesis of the current study (hypothesis B).

cortical thickness, and cross-sectional geometric properties. Examinations of wild-shot animals, as opposed to animals raised and exercised in laboratory conditions, may provide a more accurate representation of natural loading conditions. Furthermore, some artiodactyls and perissodactyls are reported to have limb skeletons that exhibit markedly less cortical remodeling than homologous human bones (Foote, 1916; Godina, 1946; Enlow and Brown, 1956, 1958; Currey, 1984a), which suggests that a relatively larger percentage of remodeling in ungulate bones may be aimed at repairing microdamage. Consistent with previous hypotheses, we anticipated that the rib would be relatively more highly remodeled than the limb bones. Additionally, we hypothesized that the prevalence of microcracks would be equivalent between the different limb bones, but each bone would exhibit a regionally distinct structural and/or material organization that might reflect local fatigue-related adaptation.

MATERIALS AND METHODS

Tissue Preparation and Microcrack Analysis

One humerus, radius, principal metacarpal (co-ossified metacarpals III and IV), and medial proximal phalanx from the left forelimb, as well as the left sixth rib were obtained from 11 freshly killed, large, skeletally mature, male, Rocky Mountain mule deer (*Odocoileus hemionus hemionus*). The mule deer were collected by hunters in the animals' natural habitat in the mountainous terrain of northern Utah, and were selected from a sample of over 1,000 animals that had been taken to a regional abattoir. The selection criteria specified large animals with a deep-fork, four-tine antler on each side, and no evidence of dental wear associated with relatively advanced age. At the time of collection, the periosteal ("velvet") covering of the antlers had been shed and antler growth was complete, suggesting that the relatively minor amount of appendicular cortical bone that had been resorbed for antler growth would have been replenished by this stage (Banks et al., 1968; Hillman et al., 1973). Since the hunt was held nearly 4 weeks prior to the mating season, the animals had not yet participated in aggressive physical interactions characteristic of the rut (Anderson, 1981; Goss, 1983). Interviews with hunters revealed that none of the animals had run after being shot, and only one deer (#11) had sustained a potentially fracture-producing fall. This animal tumbled approximately 5 m down a steep slope and fractured the tip of one antler tine. On gross examination, no other fractures were evident.

Each bone was dissected free of soft tissue and refrigerated at 4°C in a moist state. To preclude the introduction of microcracks, the bones were not frozen. Using a fine-toothed saw and continuous water irrigation, each bone was cut transversely into segments as follows: 1) a 10-cm segment from the lateral aspect of the sixth rib, the proximal cut being made 4–5 cm distal to the rib angle; 2) a 10-cm segment from the middle third of the humerus, distal to the prominent tuberosity of the proximal diaphyseal region; 3) a 10-cm segment from the middle third of the radius (and immediately distal to the distal margin of the fenestrum formed by the radioulnar synfibrosis); 4) a 10-cm segment from the middle third of the metacarpal; and 5) a 2.5-cm segment from the middle of the proximal phalanx of the medial digit.

Using a low-speed, water-cooled, diamond-blade saw (0.3-mm blade; Exact Technologies, Oklahoma City, OK), one 2.0-cm-thick transverse segment (1.5 cm in the phalanx) was cut from the central third of each of the larger bone segments. From these smaller segments, a 0.3–0.5-cm-thick transverse section was cut for linear measurements and mineral content analysis as described below. The remaining segments were evaluated for in vivo microcracks by bulk staining in 1% basic fuchsin in absolute ethanol according to the methods of Burr and coworkers (Burr and Stafford, 1990; Burr and Hoosier, 1995) after Frost (1960). Because the cortices were thicker in the metacarpal, radius, and humerus, the infiltration time for dye penetration was increased to 72 hr.

Three 115-μ-thick transverse slices were cut transversely from the middle third of each fuchsin-dyed specimen, ground and polished on a lapidary wheel to a thickness of 80–90 μ, and mounted with microscope immersion oil (to enhance resolution) onto glass slides for examination under the light microscope. The entire cortical cross-sections of the three fuchsin-dyed slices from each bone were examined for in vivo microcracks (35 slices of each bone type, for a total of 165 slices). To ensure that the microcracks seen in our bone specimens were consistent with those described by previous investigators, we examined in vivo and artifactual microcracks in several thin slices used by Burr and Stafford (1990) (provided by D.B. Burr). All slices were independently examined under the microscope by one of the current authors and two trained

laboratory assistants. Before inclusion in the data set, all putative microcracks were reviewed independently by two of the authors. Each putative microcrack had to exhibit a distinct increase of fuchsin staining along its margins (Frost, 1960; Burr and Stafford, 1990), and was included only if a consensus for inclusion was reached. Since information about microcrack initiation, propagation, and arrest can be inferred from local histomorphologic features (Martin and Burr, 1982; Burr and Martin, 1993; Norman and Wang, 1997), detailed drawings were made of the local microstructure surrounding each microcrack, including: mature secondary osteons, osteon cement lines, primary and secondary interstitial bone, forming secondary osteons, resorption spaces, primary osteons, and vascular spaces. Length measurements, which included notable changes in crack direction, were made of each microcrack at 250×.

The entire cortical area of one section of each bone from seven animals (35 sections in total) was examined for secondary osteons and new remodeling events (NREs; newly forming secondary osteons and resorption spaces), which were counted and subsequently recorded onto enlarged drawings. Secondary osteons were identified from primary osteons by their generally increased stain uptake, crenulated cement lines, and differences in birefringence under polarized light around their margins with respect to surrounding bone. The secondary osteon counts included: 1) complete secondary osteons, 2) partially formed osteons in which the entire circumference of the preceding resorption space was lined with new bone, and 3) osteon fragments with a complete central canal. Central canals were considered part of the osteon. Secondary osteon population density (OPD) refers to the number of secondary osteons per mm^2 of bone.

Cortical Thickness and Geometric Properties

Using the 0.3–0.5-cm-thick segment removed prior to bulk staining, the following measurements were made with a digital vernier caliper (Mitutoyo, Kawasaki, Japan): 1) maximum overall (subperiosteal) cranial–caudal and medial–lateral widths; and 2) cortical thickness at the cranial, caudal, medial, and lateral aspects. Drawings of these sections were traced with a digitizing pen and pad (model 12 × 12; Kurta Corp., Phoenix, AZ). An adapted version of the computer program SLICE (Nagurka and Hayes, 1980) was used to determine the 1) total subperiosteal area (TA), 2) cortical area (CA), and 3) major axis (Imax) and orthogonal minor axis (Imin) of the second moment of area (inertia, I). The CA:TA ratio and the polar moment of inertia (J = sum of moments of inertia along the major axis [Imax] and orthogonal minor axis [Imin]) were calculated for each section. According to engineering principles, 1) the total cross-sectional area (excluding the medullary cavity) in beam-like structures (such as some bones) provides an estimate of axial compressive or tensile strength, 2) the CA:TA ratio provides an estimate of robusticity, 3) J is indicative of a beam's torsional rigidity, and 4) the Imax:Imin ratio provides information about the cross-sectional shape and distribution of the material (Ruff, 1981, 1989; Ruff and Hayes, 1983; Swartz, 1993). The Imax:Imin ratio indicates the degree to which the bone cross section deviates from the purely circular. If this ratio differs substantially from one, then the whole bone strength index (see below) will not accurately estimate bending strength if the loads in the directions of Imax and Imin are not directly proportional to I in these two directions. In the present study, this may be applicable to the radius. Measured and calculated geometric parameters, including section moduli (see below), were determined for both the radius and ulna, and for the radius only. This was done to determine whether or not the presence of the ulna at mid-diaphysis significantly affected any of the correlations described below.

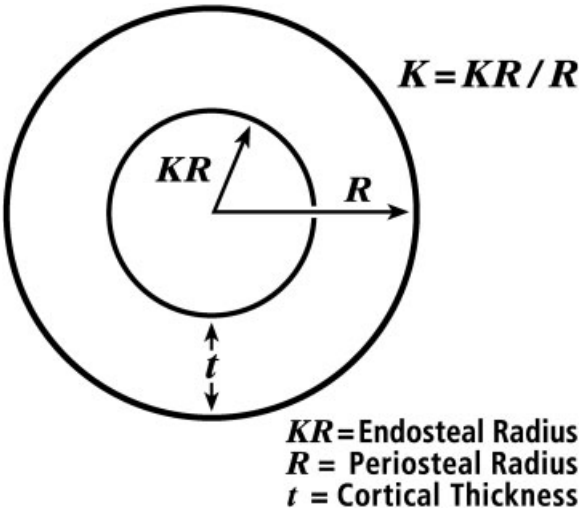

Fig. 3. Diagrammatic illustration of the measurements used to calculate the quantity *K*. See text for further description and discussion.

***K* values for estimating optima for bone bending strength.** Figure 3 represents a section through a tubular bone of radius R and cortical thickness *t*. Following Currey and Alexander (1985), the marrow cavity has radius *K*R, where the factor *K* could have any value from zero (for a solid bone) to very nearly one (for a bone with a very thin wall). The thinner the wall of the bone (the larger the value of *K*), the lighter the bone can be made. Alexander (1996, p. 19) showed that the total mass of the bone + marrow approaches a minimum where $K = 0.63$, and noted that "[a] marrow-filled bone with $K = 0.63$ is only 10% lighter than a solid bone of the same strength, and only very slightly lighter than equivalent bones with $K = 0.4$ or 0.7." In the present study, *K* values of each bone were determined to see whether they fell within this range. A more complex analysis (e.g., section modulus) is needed when bone cross-sections have different shapes.

Section modulus and whole-bone strength index. The cross-sectional strength of a bone can be characterized as the bending or torsional moment required to cause fracture. These ultimate moments are approximately proportional to the section modulus, Z, which can be calculated from the dimensions of the section (van der Meulen et al., 1996; Alexander, 1998):

$$Z = J/D$$

where J is the polar moment of inertia, and D is the mean diameter of the cross-section.

A whole-bone strength index (BSI) can be defined as:

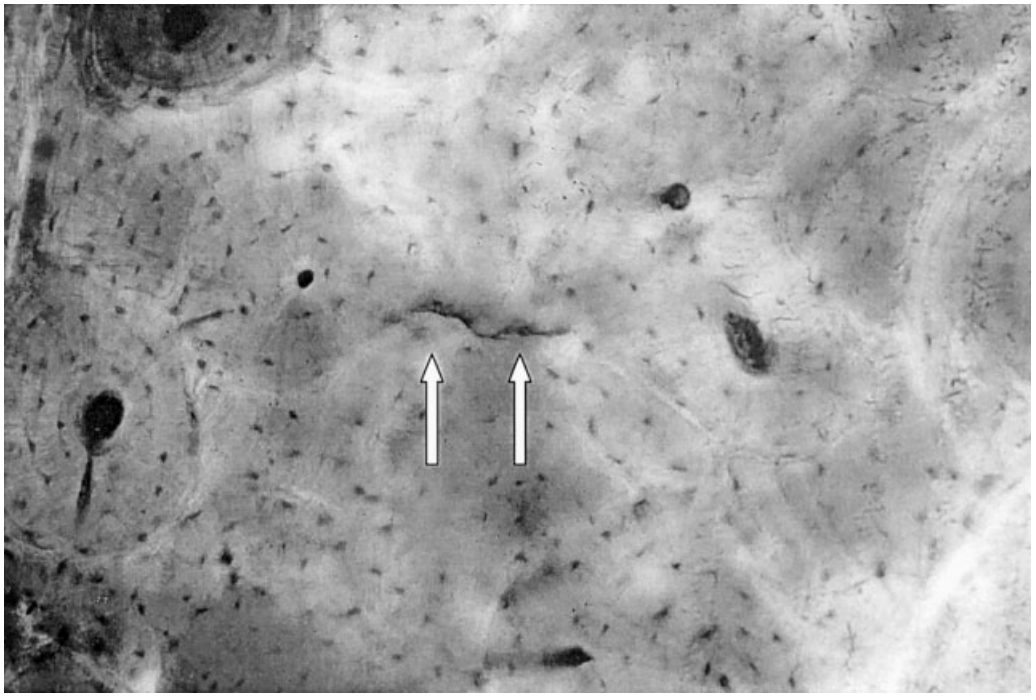

Fig. 4. Representative photomicrograph of a microcrack (arrows) in one of the rib sections (microcrack chord length = 130 μ).

$$BSI = J/DL = Z/L$$

where L is bone length in centimeters. The whole-bone strength index is proportional to the ultimate stress required to fracture a bone when it is held by its ends and a transverse force is applied at mid-diaphysis (van der Meulen et al., 1996).

Radii of Gyration

The radii of gyration were estimated at mid-diaphyses of the proximal medial phalanx, metacarpal, radius, and humerus in four freshly killed animals. This was accomplished by manually moving the forelimb of each animal through the positions of a galloping gait sequence, as shown in the cinematographic frames of Rue (1997), and measuring the radius of gyration of each bone at mid-stance, with the glenohumeral joint as the center of rotation.

Mineral Content

Pieces of bone measuring 0.3–0.4 cm in transverse width, and spanning the entire cortex, were cut from the cranial, caudal, medial, and lateral cortices at the locations where the cortical thickness measurements were made in unstained segments. These specimens were ashed to determine mineral content (Skedros et al., 1993b). Mineral content (%ash) was determined by dividing the weight of the ashed bone (W_{ab}) by the weight of the dried, defatted bone (W_{db}), and multiplying this number by 100 [(W_{ab}/W_{db}) · 100]. Mineral content by ashing is highly correlated with "specific mineralization" or "true tissue density" (g/cc) (Martin and Burr, 1989; Skedros et al., 1993a; Hernandez et al., 2001).

Statistical Analysis

Fisher's least-significant difference, one-way analysis of variance (ANOVA) tests were used to assess pairwise comparisons for statistical significance. Correlation coefficients (r values) were determined using Pearson or Spearman's correlations, as indicated.

The magnitudes of correlation coefficients were interpreted according to the classification of Hinkle et al. (1979). In this scheme, coefficients in the ranges of 0.9–0.99, 0.7–0.89, 0.5–0.69, 0.3–0.49, and 0.0–0.29 are interpreted as representing very high, high, moderate, low, and little if any correlations, respectively.

RESULTS

Microcracks

Two microcracks were identified in the limb bones (both in a single section of a radius), and 13 microcracks were found in the rib sections. Mean microcrack lengths ranged from 64.6 ± 26.0 μm (ribs) to 82.5 ± 31.8 μm (radius), and were within the range of absolute microcrack lengths (when measured in transverse sections) that have been reported in other artiodactyl species (as reviewed in Taylor and Lee, 1998). A representative microcrack is shown in Figure 4. The animal that had fallen (#11) did not show an increased prevalence of microcracks. Only one of the 15 microcracks did not touch or enter a secondary osteon or cement line, but all microcracks were within 100 μ of a secondary osteon. One microcrack was seen to course only through interstitial bone, and one microcrack was seen to course only through secondary osteonal bone.

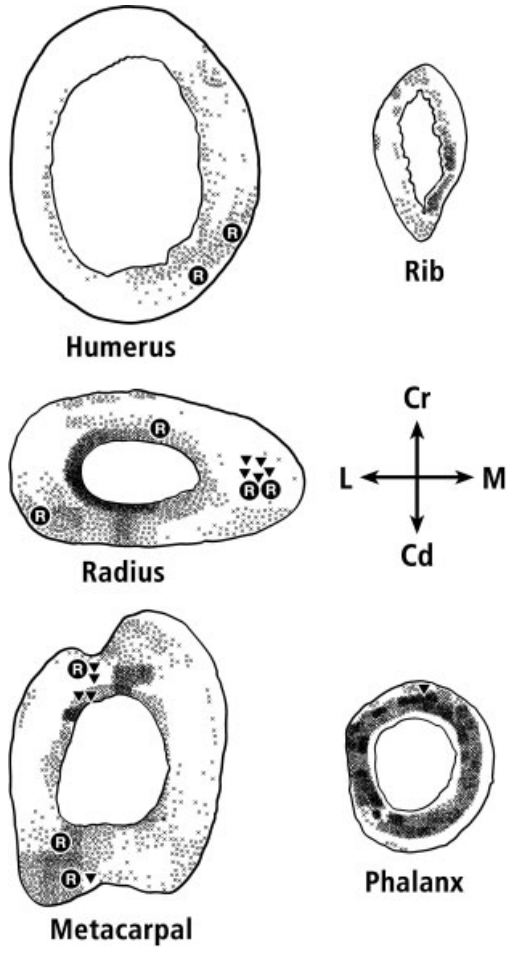

Fig. 5. Transverse sections of the bones examined in one animal. X = secondary osteons, R = resorption spaces, and triangles = newly forming osteons. Secondary osteons typically occupy approximately 30% or less of the mid-diaphyseal cortex of the principal metacarpal, radius, and humerus.

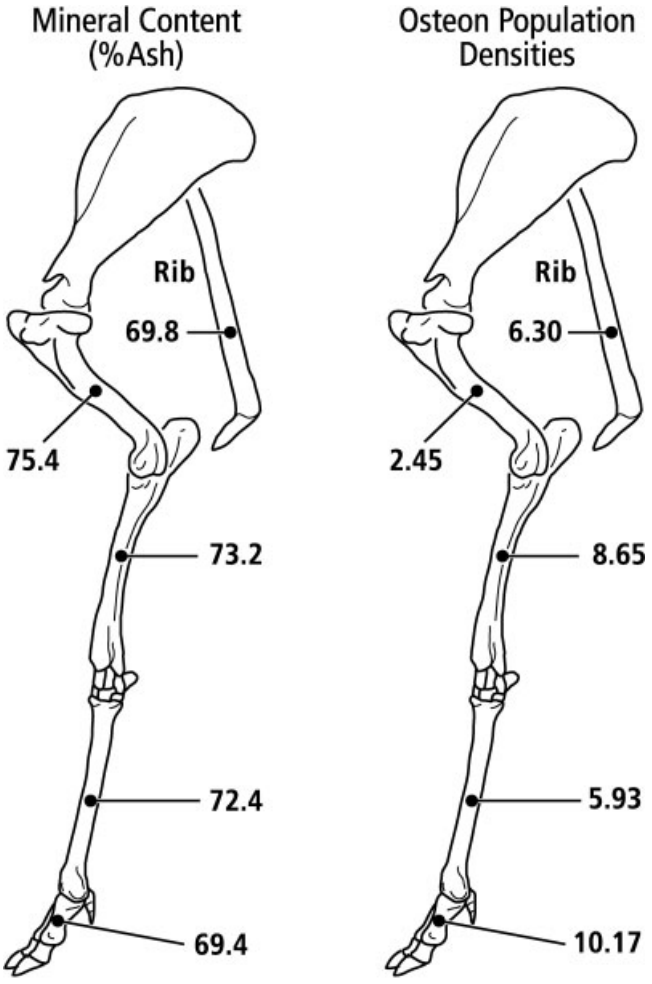

Fig. 6. Deer forelimb and rib bones showing mean mineral content (%ash) and mean OPD (no./mm^2) results.

Microstructure (Figs. 5 and 6; Table 1)

In the mid-diaphyseal sections, most of the bones were typically incompletely remodeled with secondary osteons (Fig. 5). The primary bone histology of the metacarpal, radius, and humerus was typically of the plexiform type (Enlow and Brown, 1956, 1958; Stover et al., 1992).

With OPD highest in the digit, there was some evidence of a general proximal-to-distal (phalanx to humerus, or rib) increase in OPD between bones of the appendage (Fig. 6). No significant differences in population densities of NREs were found between the different limb bones ($P > 0.2$).

Mineral Content, Cortical Thickness, and Geometric Properties (Fig. 6; Tables 1 and 2)

In concert with the OPD data, mineral content was highest in the humerus and progressively decreased to the lowest level in the digit. This decrease was statistically significant between most paired comparisons of adjacent limb bones, with absolute differences as follows: rib vs. humerus (5.6% difference, $P < 0.0001$); humerus vs. radius (2.2% difference, $P < 0.0001$); radius vs. metacarpal (0.8% difference, $P = 0.08$); and metacarpal vs. phalanx (3.0% difference, $P < 0.0001$). The mineral contents of the proximal phalanges and the ribs were not significantly different (0.5% difference; $P > 0.3$). Although general proximal-to-distal decreases were seen for J and Z, no similar changes were observed for cortical thickness and CA/TA. Values for the quantity K (ratio of endosteal-to-periosteal radius or diameter) were similar for the phalanx, metacarpal, and radius ($P > 0.3$), with the humerus being 23% higher ($P < 0.0001$) than the other three limb bones.

Correlation and Regression Analyses (Fig. 7; Tables 3 and 4)

Correlations were conducted with and without rib data. In the limb bones (excluding ribs), the polar moment of inertia (J) was highly correlated with OPD ($r = -0.708$; $P < 0.0001$) and mineral content ($r = 0.827$; $P < 0.0001$) (comparisons with section modulus (Z) were similar), and CA/TA was moderately correlated with OPD ($r = 0.621$;

TABLE 1. Microstructure and mineral content (%ash) data (Means and SD)

	Microstructure		%Ash				
	OPD[a]	NREs[b]	Mean[c]	Cranial	Caudal	Lateral	Medial
Rib	6.30 (2.54)	0.09 (0.06)	69.8 (1.0)	69.3 (1.7)	68.9 (1.4)	70.1 (1.2)	70.9 (1.5)
Humerus	2.45 (1.90)	0.04 (0.08)	75.4 (0.9)	74.8 (1.0)	74.6 (1.2)	76.0 (0.9)	76.1 (0.9)
Radius	8.65 (2.94)	0.03 (0.02)	73.2 (1.1)	73.1 (1.3)	72.5 (1.3)	73.5 (1.1)	73.5 (1.0)
Metacarpal	5.93 (2.51)	0.03 (0.02)	72.4 (1.1)	74.0 (1.0)	70.4 (1.2)	72.4 (1.2)	72.7 (1.3)
Phalanx	10.17 (2.23)	0.01 (0.01)	69.4 (1.1)	68.7 (0.9)	69.1 (1.6)	69.1 (1.8)	70.6 (0.9)

[a]OPD, Secondary osteon population density (no./mm^2).
[b]NREs, new remodeling events.
[c]Mean, average of all ashed samples from each bone.

$P < 0.001$) and mineral content ($r = -0.516$; $P < 0.001$) (Table 3, A). The OPD was moderately correlated with mineral content ($r = -0.655$; $P < 0.001$). The inclusion of the rib data substantially decreased the aforementioned correlation coefficients (Table 3, B). Representative scatterplots are provided in Figure 7.

When limb bones were assigned ordinal values indicating bone location (i.e., phalanx = 1, humerus = 4), bone location was highly correlated with mineral content ($r = 0.896$; $P < 0.0001$) and J ($r = 0.770$; $P < 0.0001$), and moderately correlated with OPD ($r = -0.609$; $P < 0.01$) (Table 4). Correlations were similarly high when the mean radius of gyration was compared to these variables. When the rib was included (value = 5), all correlations with location markedly decreased (Table 4). The inclusion of data from both the radius and ulna resulted in negligible changes in all correlated comparisons.

DISCUSSION

The results showed a significant progressive decrease in %ash from the humerus (75.4% ± 0.9%) to the phalanx (69.4% ± 1.1%) ($P < 0.0001$), accompanied by general proximal-to-distal increases in OPD and general decreases in J and Z. The progressive proximal-to-distal decrease in mineral content (absolute differences of up to 6%) suggests that material properties differ significantly between locations. This is supported by data showing that small mineral content differences in cortical bone (e.g., 3–4% absolute ash content differences) can result in large changes in mechanical properties, including fracture stress (Vose and Kubala, 1959), bending strength (Currey, 1969), impact stress (Currey, 1969, 1984a), fatigue life (Carter and Hayes, 1976), and elastic modulus (Currey and Butler, 1975; Currey, 1984b, 1988; Currey and Pond, 1989; Brear et al., 1990; Hernandez et al., 2001). Such %ash differences are similar to those found between some of the adjacent limb bones in the present study (Table 1).

The low, relatively similar occurrence of microcracks observed in the limb bones of the present study suggests that deer limb bones may be adapted for local fatigue requirements. The possibility that these specimens are also in remodeling equilibrium (i.e., no net calcium loss or gain) is supported by the absence of significant differences in NREs. A low incidence of microcracks/NREs has been demonstrated in limb bones of younger, skeletally mature humans (Schaffler et al., 1995); however, it is necessary to conduct more rigorous analyses to detect other forms of microdamage (Boyce et al., 1998; Burr et al., 1998), and to sample larger volumes of bone to further substantiate these possibilities. Although the progressive, proximal-to-distal decrease in %ash may represent regional differences in material adaptations, it is not clear whether these differences are primary adaptations or they are a secondary consequence of some other adaptation. The possibility that osteonal remodeling produces the %ash differences observed in the present study is supported by the moderate correlation between these parameters ($r = -0.655$; $P < 0.001$).

However, a causal link between OPD and %ash may be confounded by regional differences in the relative amount of remodeled bone in the locations that were sampled for mineral content, since 1) the OPD data used in the correlation analyses were obtained from the entire cross section, while the %ash data were obtained from four discrete cortical locations (cranial, caudal, medial, and lateral); 2) osteons occur in local concentrations in some of the limb bones (Fig. 5); and 3) secondary osteonal bone typically has lower mean tissue age and hence lower mineral content than primary plexiform bone (Currey, 1975, 1984a; Martin and Burr, 1989). However, the %ash data from each cortical region demonstrate rather homogenous mineral content in each bone (Table 1). This suggests that the progressive decrease in mineral content from the humerus to the phalanx may not be completely attributable to remodeling, even though this association is typically the most parsimonious explanation for mineral content differences within or between mature bones at mid-diaphysis (Marotti, 1976; Grynpas, 1993). Alternatively, the bones examined in the present study may exhibit differences in the duration (and hence the amount) of mineral accumulation, which are independent of osteon remodeling activity. In turn, such regional variations in %ash, and perhaps other structural or material characteristics, may derive more from the systematic expression of genetically derived positional information than from any individual effects of strain transduction (Rubin et al., 1992; Lovejoy et al., 2002). As noted by Lovejoy and coworkers (2002), this is supported by data showing that external bone morphology is largely dictated by an integrated system of sequentially expressed gene arrays that coordinate limb development by assigning the positional address.

Differences in modeling and remodeling rates between different limb bones and limb bone regions can also confound attempts to interpret our data in a mechanical context (Marotti, 1976). For example, if the distal bones of the deer forelimb mature (i.e., reach adult compacta) earlier than the proximal elements, this could explain the proximal-to-distal OPD gradient, since the distal bones would have more time to accumulate microdamage. There may also be differences in modeling/remodeling thresh-

TABLE 2. Geometric properties (Means and SD)

	Phalanx	Metacarpal	Radius	Radius,Ulna	Humerus	Rib
Imax/Imin	1.43 (0.15)	1.58 (0.29)	3.23 (0.44)	2.23 (0.26)	1.46 (0.13)	4.21 (1.13)
J (mm^4)	2872.52 (472.01)	20306.93 (4203.87)	17885.83 (3092.51)	21760.94 (3619.35)	27594.72 (5426.38)	1152.56 (519.14)
Z (mm^3)	229.17 (31.33)	972.86 (157.82)	897.18 (117.10)	1091.74 (132.19)	1140.95 (157.96)	103.21 (50.80)
BSI (mm^2)	4.80 (0.60)	4.37 (0.69)	3.69 (0.44)	4.49 (0.50)	5.26 (0.68)	NA
Cortical area (mm^2)	103.93 (10.81)	268.96 (24.81)	248.35 (19.04)	299.31 (36.75)	278.27 (23.73)	48.25 (13.36)
Total area (mm^2)	136.75 (11.76)	358.01 (38.24)	314.43 (27.70)	337.04 (44.31)	446.87 (47.15)	82.36 (18.11)
CA/TA (%)	76.06 (5.22)	75.28 (3.06)	79.09 (2.81)	79.90 (2.73)	62.46 (3.45)	58.26 (5.58)
Cr-Cd diameter (mm)	13.02 (0.64)	22.93 (2.14)	13.85 (0.83)	13.85 (0.83)	26.37 (1.55)	14.68 (1.52)
M-L diameter (mm)	11.96 (0.50)	18.53 (0.74)	25.82 (1.57)	25.82 (1.57)	21.69 (1.18)	7.81 (2.55)
Cr-Cd/M-L diameter ratio	1.09 (0.05)	1.24 (0.13)	0.54 (0.04)	0.54 (0.04)	1.22 (0.03)	1.90 (0.29)
K	0.51 (0.04)	0.53 (0.03)	0.49 (0.04)	0.49 (0.04)	0.63 (0.04)	0.64 (0.05)
Cortical thickness (mm)	3.08 (0.29)	4.91 (0.33)	4.95 (0.48)	4.95 (0.48)	4.46 (0.49)	1.83 (0.20)

Imax/Imin, ratio of the axes of the second moments of inertia (area); J, polar moment of inertia; Z, section modulus; BSI, whole bone strength index; CA, cortical area; TA, total subperiosteal area; Cr-Cd, cranial-caudal; M-L, medial-lateral; *K*, ratio of endosteal-to-periosteal radius; NA, not applicable.

Fig. 7. Representative scatterplots.

olds between limb bones and limb bone regions (Marotti, 1976; Hsieh et al., 2001). We must gain a more thorough understanding of the modeling/remodeling rates and thresholds for the various limb bones in order to further examine these possibilities.

Some Gait Patterns May Produce Nonprogressive Peak Stress/Strain Magnitudes

If the majority of the remodeling in the deer bones is directed toward repairing microdamage, then the distribution and concentration of secondary osteons may reflect a corresponding history of microcrack formation and repair. The proximal-to-distal OPD variations may therefore reflect similar variations in habitual or peak stresses and strains. This is possible because stresses, and hence strains, imparted to limb bones depend on many factors, including 1) locomotor speed and nature of gait, 2) posture of the animal and limb, 3) bone curvature and cross-sectional shape, and 4) biomechanics of associated tendons and muscles. For example, Biewener et al. (1983) showed that during certain gaits and jumping, strains in the equine radius can exceed those in the more-distal principal metacarpal. They attributed this to more prevalent eccentric loading of the longitudinally curved radius. Proximal-to-distal variations in peak stresses may explain the OPD pattern shown in the present study (Fig. 6). This idea is similarly based on the possibility that the radius receives greater stresses than the metacarpal during some common gait-related activities, because the radius has longitudinal curvature and is narrowed in the direction of bending, and because relatively greater forces may also occur in this bone during the "bounding" gaits ("pronking" or "stotting," and the eight-step rotary gait of a full gallop)

TABLE 3. Pearson correlation coefficients (r values), (n = 11 animals)

	OPD[a]	NREs[a]	%Ash	Cortical T	CA/TA	J	J px2	Z	Z px2	BSI
A. Excluding rib data										
OPD[a]	1.000									
NREs[a]	−0.085	1.000								
%Ash	−0.655[c]	0.346	1.000							
Cortical T	−0.306	0.267	0.588[b]	1.000						
CA/TA	0.621[c]	−0.031	−0.516[c]	0.102	1.000					
J	−0.708[b]	0.185	0.827[b]	0.710[b]	−0.555[b]	1.000				
J px2	−0.709[b]	0.172	0.813[b]	0.672[b]	−0.589[b]	0.997[b]	1.000			
Z	−0.664[c]	0.195	0.819[b]	0.779[b]	−0.450[c]	0.987[b]	0.974[b]	1.000		
Z px2	−0.665[c]	0.168	0.795[b]	0.718[b]	−0.509[c]	0.991[b]	0.990[b]	0.987[b]	1.000	
BSI	−0.321	−0.105	0.125	−0.209	−0.583[b]	0.318[d]	0.391[c]	0.206	0.353[d]	1.000
B. With rib data										
OPD[a]	1.000									
NREs[a]	0.020	1.000								
%Ash	−0.533[c]	−0.074	1.000							
Cortical T	−0.117	−0.320	0.667[b]	1.000						
CA/TA	0.473[c]	−0.397[d]	−0.051	0.541[b]	1.000					
J	−0.508[c]	−0.215	0.849[b]	0.811[b]	0.044	1.000				
J px2	−0.475[c]	−0.259	0.832[b]	0.820[b]	0.082	0.995[b]	1.000			
Z	−0.434[d]	−0.244	0.833[b]	0.869[b]	0.162	0.989[b]	0.984[b]	1.000		
Z px2	−0.353[d]	−0.336[d]	0.786[b]	0.882[b]	0.253	0.965[b]	0.980[b]	0.979[b]	1.000	

[a]n = 7 animals.
[b]$P < 0.0001$.
[c]$P < 0.005$.
[d]$P < 0.05$, all other correlations: $P > 0.05$
OPD, Secondary osteon population density; NREs, New remodeling events; Cortical T, Cortical thickness; CA/TA, Cortical area/total area; J, Polar moment of inertia; Z, Section modulus; BSI, Whole bone strength index; J px2 and Z px2, indicate that data were doubled for the phalanx.

TABLE 4. Spearman correlations: variables vs location and radius of gyration (n = 11 animals)

	OPD[a]	NREs[a]	%Ash	Cortical T	CA/TA	J	Z
Location (excluding rib)	−0.609[c]	−0.148	0.896[b]	0.431[c]	−0.431[c]	0.770[b]	0.719[b]
Location (with rib data)	−0.448[c]	0.519[c]	0.274[d]	−0.232	−0.674[b]	−0.044	−0.061
Radius of gyration	−0.609[c]	0.148	−0.896[b]	−0.431[d]	0.431[c]	−0.770[b]	−0.719[b]

Location refers to ordinal values assigned to each bone from distal to proximal. Radius of gyration (mean), center of glenohumeral articulation to mid-diaphysis of each bone: prominal medial phalanx (73.0cm), principal metacarpal (58.4cm), radius (31.8cm), and humerus (11.4cm).
[a]n = 7 animals
[b]$P < 0.0001$.
[c]$P < 0.01$.
[d]$P \leq 0.05$; all other correlations: $P > 0.05$.
OPD, Secondary osteon population density; NREs, New remodeling events; Cortical T, Cortical thickness; CA/TA, Cortical area/total area; J, Polar moment of inertia; Z, Section modulus.

common to this deer and other artiodactyl species (Hildebrand, 1977; Rue, 1997; Hildebrand and Goslow, 2001). Additionally, the metacarpal is generally more robust geometrically than the radius (Table 2). Similar arguments may also help to explain why, in the same limb of normal, 2-year-old thoroughbred horses, cortical bone from the radius has greater impact strength than cortical bone from the third metacarpal (Reilly et al., 1997; Batson et al., 2000).

Remodeling and Microdamage Repair

In experimental studies using bovine bone, Currey (1975) and Carter et al. (1976) showed that primary bone is stronger and more fatigue-resistant than more extensively remodeled bone. They attributed these results to the presence of secondary osteons, which reduce mineral content by reducing mean tissue age and increasing porosity, respectively, and create an inherently weaker structure by increasing cement line and lamellar interfaces. However, more recently investigators have recognized the capacity of secondary bone to attenuate microcrack propagation (Martin and Burr, 1989; Reilly et al., 1997; Reilly and Currey, 1999; Yeni and Norman, 2000), which may be a consequence of these interfaces. While the best way to avoid fatigue failure may be to decrease microcrack incidence, Martin et al. (1998) argued that bone that is highly resistant to microdamage initiation will be inefficient at controlling microcrack propagation. The trade-off for highly stressed, fatigue-prone bone, therefore, may be efficient repair and a decrease in propagation, rather than prevention of microcrack initiation (Reilly et al., 1997). Studies have suggested that secondary osteonal bone is rather poor at minimizing microcrack formation, but rather good at attenuating the distance and rate of

microcrack propagation (Reilly et al., 1997; Taylor, 1997; Burr et al., 1988; Martin et al., 1998; Reilly and Currey, 1999). In the bones examined in the present study, regional disparities in microcrack incidence (i.e., lowest in the humerus and greatest in the phalanx) may have been present earlier in skeletal ontogeny, which suggests that strain thresholds above which microdamage is produced were more likely exceeded in distal than in proximal bones. Remodeling may have subsequently eliminated these disparities, raised strain-related microdamage thresholds, and produced the observed regional OPD differences. In turn, the current microcrack incidence in these mature bones may be negligibly low, in contrast to the relatively higher frequency that is probably seen earlier in ontogeny. Further studies in an ontogenetic series of animals are needed to clarify these issues.

The greater number of microcracks observed in ribs may reflect the 1) relatively high OPD and increased remodeling rate, which results in increased porosity, decreased mineral content, and increased cement lines; 2) seasonal remodeling events in ribs, sterna, and vertebrae, which provide the majority of mineral for antler growth (Meister, 1956; Banks et al., 1968; Hillman et al., 1973; Goss, 1983; Baksi and Newbrey, 1989; Bubenik, 1990); and/or 3) increased loading cycles (which are an important determinant in the formation of fatigue microdamage (Parfitt, 2002)) resulting from thoracic breathing motion, which occurs both when the animal is recumbent and when it is ambulating. Seasonal osteonal remodeling in the ribs, therefore, produces structural weakness, which may increase the probability of microcracking under physiologic loads. As noted by Currey (1981), the ribs, in contrast to weight-bearing limb bones, can afford the potential reduction in strength resulting from increased remodeling, reduced mineral content, and increased microcrack prevalence. Thus, the ribs probably can function effectively with a proportionately lower safety factor than the limb bones.

Although the lower functional demand on ribs allows mineral resorption during the metabolically demanding process of antler growth, such mineral requisition via remodeling is not exclusive to the ribs. In addition to the ribs, Hillman et al. (1973) also demonstrated some remodeling in the principal metatarsals and metacarpals of mule deer during peak antler growth. Therefore, some of the secondary osteons seen within limb bones in the present study may not have been aimed at repairing microcracks. Female animals were not used in this study because appendicular bone remodeling may be even greater as a result of the mineral demands of pregnancy and lactation. Although previous studies suggested that the vast majority of seasonal mineral resorption in males occurs in the ribs, sternum, and vertebrae, antler growth may partially confound interpretations that attempt to draw a link between microdamage and OPD. Since a comparatively small percentage of the metacarpal, radius, and humerus sections are remodeled with secondary osteons (Fig. 5), we suggest that these bones probably have relatively larger proportions of osteons that were aimed at microdamage repair compared to species exhibiting more extensively remodeled cortices (Foote, 1916; Enlow and Brown, 1958; Enlow, 1962; Singh et al., 1974; Richman et al., 1979; Bell et al., 2001). Although there are cogent theoretical arguments supporting the idea that the majority of osteonal remodeling seen in deer and other terrestrial mammals is directed at microdamage repair (Martin, 2002), the fact that this idea remains controversial (Parfitt, 2002; Burr, 2002) bespeaks the need for further studies.

Modeling vs. Remodeling—Compensation, Trade-Offs, and Developmental Constraint

Minimizing mass in the distal limb helps conserve angular momentum, and hence mechanical work during gait (Steudel, 1990a, b; Walker and Liem, 1994; Alexander, 1998). Distal mass is reduced by tapering the limbs—maintaining muscle bellies proximally, and having long tendons course distally (Hildebrand and Hurley, 1985; Steudel, 1990a, b). Mass reduction in the appendicular skeleton is also important, and is readily achieved by structural modifications produced by modeling activities. Theoretically, remodeling activities (i.e., the formation of secondary osteons) may also help to reduce distal bone mass. Synergism between modeling and remodeling activities in this context is implied in the present study by the high correlation between %ash (a material characteristic) and J (a structural characteristic). Although such "synergism" seems unlikely in adult animals (see below), a "compensatory" interaction between modeling-mediated adjustments in structural strength/geometry, and remodeling-mediated changes in bone density has been suggested in studies of the femur and humerus of aging humans from modern and archaic populations (Martin and Atkinson, 1977; Martin et al., 1980; Burr et al., 1990). Burr et al. (1981) suggested that similar associations in relatively distal locations of macaque and human femoral diaphyses may maintain structural strength at an optimal level without increasing tissue density. Since the humerus of mammals is almost always larger than the radius, which is larger than the principal metacarpal, etc., J will show a proximal-to-distal gradient. Consequently, correlations with proximal-to-distal variations in cross-sectional geometric properties may be circumstantial, not causal or synergistic. Hence, the most significant finding in the present study may be the proximal-to-distal gradients in the material characteristics. Clearly, future studies designed to more rigorously address these questions will require, at the least, estimates of the stress magnitudes developed in each of the limb bones, based on load magnitude and orientation, mechanical properties, and structural geometry.

Lieberman and Crompton (1998) reported a similar interpretation in their studies of immature pigs. They showed that compared to proximal limb bones (humerus or femur), distal limb bones (principal metacarpal or metatarsal) apparently conserve mass by modeling less, but maintain reduced mass with higher remodeling rates (which reduce mean tissue age and increase porosity). This pattern was exaggerated in immature exercised animals, in which remodeling rates increased in proportion to the square of each bone's mid-diaphyseal radius of gyration (Lieberman and Crompton, 1998). Similar nonlinear relationships between the radius of gyration with mineral content, OPD, and NREs were not found in the mature animals examined in the present study.

Previous studies (Pearson and Lieberman, 2002) suggested that limb bones of mature sheep undergo remodeling (greater in distal bone) as a means of adapting to increased stresses associated with exercise. However, such remodeling-related material adaptations (e.g., linked %ash and OPD variations) would not be expected to have

major effects on mass reduction or on structural properties such as whole-bone stiffness or strength. For example, using methods described by Hernandez et al. (2001), and assuming that the deer limb bones are cylindrical, it is possible to estimate the increased mass that would occur if the mineral contents of the principal metacarpal and all phalanges in one mule deer forelimb were increased to the %ash of the mid-diaphyseal humerus (75.4%). This would increase material density (true tissue density) by approximately 4% (2.3–2.4 g/cc). In turn, this would increase the mass of the distal forelimb by no more than 6 g. Les (1999) has shown that even a 12% increase in material density (an amount that is relatively inexpensive to move) will result in only a small increase in mass (Taylor et al., 1970, 1982; Steudel, 1990a, b). Increased resorption spaces and larger central canals of forming secondary osteons in distal limb bones of exercising animals would probably also have a minor role in mass reduction, especially since such changes are typically transient. Consequently, such material variations probably have negligible influence in optimizing bone mass, and the idea of modeling and remodeling working in a "compensatory" fashion to modify mass or structural properties seems unlikely in adult animals in natural conditions.

Modeling vs. Remodeling—Loading Predictability and Division of Labor

The progressive proximal-to-distal decrease in %ash, and the general increase in OPD shown in the mule deer forelimb may be influenced by ontogenetic constraints that restrict the relative prevalence of modeling and remodeling. In other words, modeling is the predominant means of reducing deleterious strains and modifying structure and mass during normal growth and exercise-related regimes imposed during growth (Woo et al., 1981; Nunamaker et al., 1987, 1989, 1990; Biewener and Bertram, 1993, 1994; Judex et al., 1997; Mosley et al., 1997). In contrast, modeling is uncommon in unexercised skeletally mature animals (Bertram and Swartz, 1991; Biewener and Bertram, 1994). What function, then, does osteonal remodeling serve in an adult animal, and what function does it serve prior to maturity? As suggested above, microdamage-targeted remodeling may account for a majority of the limb-bone remodeling seen throughout ontogeny in the species examined in the present study, with metabolic demands of antler growth playing a lesser role. However, it is important to emphasize that material adaptations achieved via osteonal remodeling processes would be neither required nor expected for whole-bone stiffness/strength requirements in the vast majority of cases (Woo et al., 1981; Rubin and Lanyon, 1982; Alexander, 1998). This is because a predictable, and hence controlled, strain environment is readily achieved and accommodated by modeling processes that affect structural characteristics such as bone curvature, cortical thickness, and cross-sectional moments of inertia, which in turn affect whole-bone stiffness and strength (Bertram and Biewener, 1988). Additionally, the calculated values for the quantity K (ratio of endosteal-to-periosteal radius or diameter) in the present study are similar to those previously reported for the femora, tibiae, metatarsals, humeri, and metacarpals of cursorial, unguligrade animals that have mass similar to mule deer (Currey and Alexander, 1985; Alexander, 1996). These values are also consistent with the theoretical optimum for resistance to impact loads (Currey and Alexander, 1985). This suggests that cortical modeling processes in the deer limb bones may also be directed toward whole-bone impact resistance.

It has been proposed that structural variations, such as cortical thickness differences and cross-sectional shape asymmetry, are selected for enhancing "loading predictability" during typical use (Bertram and Biewener, 1988; Swartz, 1990). In turn, a predictable strain distribution produced by loading predictability may convey fundamentally important signals for limb bone tissue/organ growth and maintenance (Bertram and Biewener, 1988; Skedros et al., 1996). Enhancing "loading predictability" may therefore be an important goal of a bone's adapted morphology (Skedros et al., 2003a). Analytical studies suggest that remodeling-related material variations, such as OPD, porosity, %ash, and predominant collagen fiber orientation, do not significantly enhance loading predictability (Gross et al., 1992; Les, 1995) (Les, personal communication). However, experimental studies have shown that some of these material characteristics can have important influences on local energy absorption, toughness, and/or fatigue resistance (Yeni et al., 1997; Jepsen et al., 1999; Brown et al., 2000; Shelton et al., 2000; Skedros et al., 2000, 2001b, 2003b, c).

CONCLUSIONS

The current results show a significant proximal-to-distal progressive decrease in %ash and a general increase in OPD, with the radius exhibiting slightly more remodeling than the metacarpus. During some gaits, eccentric loading of the limb, sagittal curvature and cross-sectional shape of the radius, and stress transfer associated with "bounding" gaits may result in relatively higher strains in the radius than in the more distal metacarpal bone. Consequently, a proximal-to-distal peak stress gradient may occur during gaits that most commonly produce microdamage. Apparent regional differences in the structural and material organization of each bone may reflect, in part, adaptations to such nonuniform stress patterns. Functional loading may play an important role in producing the putative thresholds that govern remodeling responses to normal strain environments and/or microdamage production. Although the causal mechanisms that produce the structural and material patterns shown in the present study are not known, we speculate that material variations have a negligible influence on optimizing bone mass or whole-bone structural properties. Rather, it is probable that these material variations secondarily enhance regional, stress/strain-related differences in fatigue resistance, toughness, and/or energy absorption.

ACKNOWLEDGMENTS

The authors thank C. Owen Lovejoy and Phil Reno for their critical reviews; Clay and Craig Meier for their assistance in obtaining the bones used in this study; Michael Fink, Alidad Ghiazzi, and Geoff Leung for technical support; and Kerry Matz for illustrations.

LITERATURE CITED

Alexander RM. 1996. Optima for animals. Princeton: Princeton University Press. 169 p.

Alexander RM. 1998. Symmorphosis and safety factors. In: Weibel ER, Taylor CR, Bolis L, editors. Principles of animal design: the optimization and symmorphosis debate. Cambridge: Cambridge University Press. p 28–35.

Anderson AE. 1981. Morphologic and physiological characteristics. In: Walmo OC, editor. Mule and black-tailed deer of North America. Lincoln: University of Nebraska. p 27–97.

Baksi SN, Newbrey JW. 1989. Bone metabolism during antler growth in female reindeer. Calcif Tissue Int 45:314–317.

Banks WJ, Glenwood PE, Kainer RA, Davis RW. 1968. I. Morphological and morphometric changes in the costal compacta during the antler growth cycle. Anat Rec 162:387–398.

Batson EL, Reilly GC, Currey JD, Balderson DS. 2000. Postexercise and positional variation in mechanical properties of the radius on young horses. Equine Vet J 32:95–100.

Bell KL, Loveridge N, Reeve J, Thomas CDL, Feik SA, Clement JG. 2001. Super-osteons (remodeling clusters) in the cortex of the femoral shaft: influence of age and gender. Anat Rec 264:378–386.

Bertram JEA, Biewener AA. 1988. Bone curvature: sacrificing strength for load predictability? J Theor Biol 131:75–92.

Bertram JEA, Swartz SM. 1991. The 'law of bone transformation': a case of crying Wolff? Biol Rev 66:245–273.

Biewener AA, Thomason J, Lanyon LE. 1983. Mechanics of locomotion and jumping in the forelimb of the horse (*Equus*): *in vivo* stress developed in the radius and metacarpus. J Zool, Lond 201:67–82.

Biewener AA, Bertram JEA. 1993. Mechanical loading and bone growth *in vivo*. In: Hall BK, editor. Bone. Vol. 7. Bone growth, part B. Boca Raton: CRC Press. p 1–36.

Biewener AA, Bertram JEA. 1994. Structural response of growing bone to exercise and disuse. J Appl Physiol 76:946–955.

Boyce TM, Fyhrie DP, Glotkowski MC, Radin EL, Schaffler MB. 1998. Microdamage type and strain mode associations in human compact bone bending fatigue. J Orthop Res 16:322–329.

Brear K, Currey JD, Pond CM. 1990. Ontogenetic changes in the mechanical properties of the femur of the polar bear *Ursus maritimus*. J Zool Lond 222:49–58.

Brown CU, Yeni YN, Norman TL. 2000. Fracture toughness is dependent on bone location—a study of the femoral neck, femoral shaft, and the tibial shaft. J Biomed Mater Res 49:380–389.

Bubenik GA. 1990. The antler as a model in biomedical research. In: Bubenik GA, Bubenik AB, editors. Horns, pronghorns, and antlers. New York: Springer-Verlag. p 474–487.

Burr DB, Piotrowski G, Miller GJ. 1981. Structural strength of the macaque femur. Am J Phys Anthropol 54:305–319.

Burr DB, Schaffler MB, Frederickson RG. 1988. Composition of the cement line and its possible mechanical role as a local interface in human compact bone. J Biomech 21:939–945.

Burr DB, Stafford T. 1990. Validity of the bulk-staining technique to separate artifactual from *in vivo* bone microdamage. Clin Orthop Relat Res 260:305–308.

Burr DB, Ruff CB, Thompson DD. 1990. Patterns of skeletal histologic change through time: comparison of an archaic native American population with modern populations. Anat Rec 226:307–313.

Burr DB, Martin RB. 1993. Calculating the probability that microcracks initiate resorption spaces. J Biomech 26:613–616.

Burr DB, Hoosier M. 1995. Alteration to the en bloc fuchsin staining protocol for the demonstration of microdamage produced *in vivo*. Bone 17:431–433.

Burr DB, Turner CH, Naick P, Forwood MR, Ambrosius W, Hasan MS, Pidaparti R. 1998. Does microdamage accumulation affect the mechanical properties of bone? J Biomech 31:337–345.

Burr DB. 2002. Targeted and nontargeted remodeling. Bone 30:2–4.

Carter DR, Hayes WC. 1976. Fatigue life of compact bone. I. Effects of stress amplitude, temperature and density. J Biomech 9:27–34.

Carter DR, Hayes WC, Schurman DJ. 1976. Fatigue life of compact bone. II. Effects of microstructure and density. J Biomech 9:211–218.

Currey JD. 1959. Differences in the tensile strength of bone of different histological types. J Anat 93:87–95.

Currey JD. 1969. The mechanical consequences of variation in the mineral content of bone. J Biomech 2:1–11.

Currey JD. 1975. The effects of strain rate, reconstruction and mineral content on some mechanical properties of bovine bone. J Biomech 8:81–86.

Currey JD, Butler G. 1975. The mechanical properties of bone tissue in children. J Bone Joint Surg 57-A:810–814.

Currey JD. 1981. What is bone for? Property–function relationships in bone. In: Cowin SC, editor. Mechanical properties of bone. New York: American Society of Mechanical Engineers. p 13–26.

Currey JD. 1984a. The mechanical adaptations of bones. Princeton: Princeton University Press. 294 p.

Currey JD. 1984b. Effects of differences in mineralization on the mechanical properties of bone. Phil Trans R Soc Lond B 304:509–518.

Currey JD, Alexander RMcN. 1985. The thickness of the walls of tubular bones. J Zool Lond 206:453–468.

Currey JD. 1988. The effect of porosity and mineral content on the Young's modulus of elasticity of compact bone. J Biomech 21:131–139.

Currey JD, Pond CM. 1989. Mechanical properties of very young bone in the axis deer (*Axis axis*) and humans. J Zool Lond 218:59–67.

Enlow DH, Brown SO. 1956. A comparative histological study of fossil and recent bone tissues. Part I. Introduction, methods, fish and amphibian bone tissues. Tex J Sci 8:405–443.

Enlow DH, Brown SO. 1958. A comparative histological study of fossil and recent bone tissues. Part III. Mammalian bone tissues. General discussion. Tex J Sci 10:187–230.

Enlow DH. 1962. Functions of the Haversian system. Am J Anat 110:269–305.

Foote JS. 1916. A contribution to the comparative histology of the femur. Smithsonian Contributions to Knowledge 35:3. Smithsonian Institution, Washington. Baltimore: Lord Baltimore Press. 242 p.

Frost HM. 1960. Presence of microscopic cracks *in vivo* in bone. Henry Ford Hosp Med Bull 8:25–35.

Godina G. 1946. Trasformazioni strutturali della compatta delle ossa lunghe degli Equidi durante l'accrescimento e nella senescenza. Arch Ital Anat Embriol 51:219–241.

Goss RJ. 1983. Deer antlers: regeneration, function and evolution. New York: Academic Press. 316 p.

Gross TS, McLeod KJ, Rubin CT. 1992. Characterizing bone strain distributions *in vivo* using three triple rosette strain gauges. J Biomech 25:1081–1087.

Grynpas M. 1993. Age and disease-related changes in the mineral of bone. Calcif Tissue Int 53(Suppl 1):S57–S64.

Hernandez CJ, Beaupré GS, Keller TS, Carter DR. 2001. The influence of bone volume fraction and ash fraction on bone strength and modulus. Bone 29:74–78.

Hildebrand M. 1977. Analysis of asymmetrical gaits. J Mammal 58: 131–156.

Hildebrand M, Hurley JP. 1985. Energy of the oscillating legs of a fast-moving cheetah, pronghorn, jackrabbit, and elephant. J Morphol 184:23–31.

Hildebrand M, Goslow Jr GE. 2001. Analysis of vertebrate structure. 5th ed. New York: John Wiley and Sons, Inc. 654 p.

Hillman JR, Davis RW, Abdelbaki YZ. 1973. Cyclic bone remodeling in deer. Calcif Tissue Res 12:323–330.

Hinkle DE, Wiersma W, Jurs WG. 1979. Applied statistics for the behavioral sciences. Chicago: Rand McNally College Publishing Co. 489 p.

Hsieh YF, Robling AG, Ambrosius WT, Burr DB, Turner CH. 2001. Mechanical loading of diaphyseal bone *in vivo*: the strain threshold for an osteogenic response varies with location. J Bone Miner Res 16:2291–2297.

Jepsen KJ, Davy DT, Krzypow DJ. 1999. The role of the lamellar interface during torsional yielding of human cortical bone. J Biomech 32:303–310.

Judex S, Gross TS, Zernicke RF. 1997. Strain gradients correlate with sites of exercise-induced bone-forming surfaces in the adult skeleton. J Bone Miner Res 12:1737–1745.

Les CM. 1995. Material heterogeneity in the equine metacarpus: documentation and biomechanical consequences. Ph.D. dissertation, University of California–Davis. 244 p.

Les CM. 1999. Why not more dense? Wolff's law and skeletal mass. Trans Orthopaed Res Soc 24:769.

Lieberman DE, Crompton AW. 1998. Responses of bone to stress: constraints on symmorphosis. In: Weibel ER, Taylor CR, Bolis L, editors. Principles of animal design: the optimization and symmorphosis debate. Cambridge: Cambridge University Press. p 78–86.

Lovejoy CO, Meindl RS, Ohman JC, Heiple KG, White TD. 2002. The Maka femur and its bearing on the antiquity of human walking: applying contemporary concepts of morphogenesis to the human fossil record. Am J Phys Anthropol 119:97–133.

Marotti G. 1976. Map of bone formation rate values recorded throughout the skeleton of the dog. In: Jaworski ZFG, editor. Proceedings of the 1st Workshop on Bone Morphometry. Ottawa: Ottawa University Press. p 202–207.

Martin RB, Atkinson PJ. 1977. Age and sex-related changes in the structure and strength of the human femoral shaft. J Biomech 10:223–231.

Martin RB, Pickett JC, Zinaich S. 1980. Studies of skeletal remodeling in aging men. Clin Orthop Rel Res 149:268–282.

Martin RB, Burr DB. 1982. A hypothetical mechanism for the stimulation of osteonal remodeling by fatigue damage. J Biomech 15: 137.

Martin RB, Burr DB. 1989. Structure, function and adaptation of compact bone. New York: Raven Press. 275 p.

Martin RB, Burr DB, Sharkey NA. 1998. Skeletal tissue mechanics. New York: Springer-Verlag. 392 p.

Martin RB. 2002. Is all cortical bone remodeling initiated by microdamage? Bone 30:8–13.

Meister WW. 1956. Changes in histological structure of the long bones of white-tailed deer (*Odocoileus virginianus*) during the growth of the antlers. Anat Rec 124:709–721.

Mosley JR, March BM, Lynch J, Lanyon LE. 1997. Strain magnitude related changes in whole bone architecture in growing rats. Bone 20:191–198.

Nagurka ML, Hayes SC. 1980. An interactive graphics package for calculating cross-sectional properties of complex shapes. J Biomech 13:59–64.

Norman TL, Wang Z. 1997. Microdamage of human cortical bone: incidence and morphology in long bones. Bone 20:375–379.

Nunamaker DM, Butterweck DM, Black J. 1987. Fatigue fractures in thoroughbred racehorses: relationship with age and strain. Trans Orthop Res Soc 12:72.

Nunamaker DM, Butterweck DM, Provost MT. 1989. Some geometric properties of the third metacarpal bone: a comparison between the thoroughbred and standardbred racehorse. J Biomech 22:129–134.

Nunamaker DM, Butterweck DM, Provost MT. 1990. Fatigue fractures in thoroughbred racehorses: relationships with age, peak bone strain, and training. J Orthop Res 8:604–611.

Parfitt AM. 2002. Targeted and nontargeted bone remodeling: relationship to basic multicellular unit organization and progression. Bone 30:5–7.

Pearson O, Lieberman D. 2002. Effects of age and exercise on long bone modeling and remodeling. Am J Phys Anthropol 34(Suppl): 123.

Reilly DT, Burstein AH. 1974. The mechanical properties of cortical bone. J Bone Joint Surg 56-A:1001–1022.

Reilly GC, Currey JD, Goodship AE. 1997. Exercise of young thoroughbred horses increases impact strength of the third metacarpal bone. J Orthop Res 15:862–868.

Reilly GC, Currey JD. 1999. The development of microcracking and failure in bone depends on the loading mode to which it is adapted. J Exp Biol 202:543–552.

Richman EA, Ortner DJ, Schulter-Ellis FP. 1979. Differences in intracortical bone remodeling in three aboriginal American populations: possible dietary factors. Calcif Tissue Int 28:209–214.

Rubin CT, Lanyon LE. 1982. Limb mechanics as a function of speed and gait: a study of functional strains in the radius and tibia of horse and dog. J Exp Biol 101:187–211.

Rubin CT, McLeod KJ, Gross TS, Donahue HJ. 1992. Physical stimuli as potent determinants of bone morphology. In: Carlson DS, Goldstein SA, editors. Bone biodynamics in orthodontic and orthopedic research. Ann Arbor: University of Michigan. p 75–91.

Rue LL. 1997 The deer of North America. New York: Lyons Press. 544 p.

Ruff CB. 1981. Structural changes in the lower limb bones with aging at Pecos Pueblo. Ph.D. dissertation, University of Pennsylvania, Philadelphia. 492 p.

Ruff CB, Hayes WC. 1983. Cross-sectional geometry of Pecos Pueblo femora and tibiae—a biomechanical investigation. I. Method and general patterns of variation. Am J Phys Anthropol 60:359–381.

Ruff CB. 1989. New approaches to structural evolution of limb bones in primates. Folia Primatol 53:142–159.

Schaffler MB, Choi K, Milgrom C. 1995. Aging and microdamage accumulation in human compact bone. Bone 17:521–525.

Shelton DR, Gibeling JC, Martin RB, Stover SM. 2000. Fatigue crack growth rates in equine cortical bone. In: Proceedings of the 24th Annual Meeting of the American Society of Biomechanics, Chicago. p 247–248.

Singh IJ, Tonna EA, Gandel CP. 1974. A comparative histological study of mammalian bone. J Morphol 144:421–438.

Skedros JG, Bloebaum RD, Bachus KN, Boyce TM. 1993a. The meaning of graylevels in backscattered electron images of bone. J Biomed Mater Res 27:47–56.

Skedros JG, Bloebaum RD, Bachus KN, Boyce TM, Constantz B. 1993b. Influence of mineral content and composition on graylevels in backscattered electron images of bone. J Biomed Mater Res 27:57–64.

Skedros JG, Mason MW, Nelson MC, Bloebaum RD. 1996. Evidence of structural and material adaptation to specific strain features in cortical bone. Anat Rec 246:47–63.

Skedros JG, Dayton MR, Bachus KN. 2000. Relative effects of collagen fiber orientation, mineralization, porosity, and percent and population density of osteonal bone mechanical properties in mode-specific loading. In: Proceedings of the 24th Annual Meeting of the American Society of Biomechanics, Chicago. p 173–174.

Skedros JG, Hunt KJ, Dayton MT, Bloebaum RD, Bachus KN. 2001a. Relative contributions of material characteristics to failure properties of cortical bone in strain-mode-specific loading: implications for fragility in osteoporosis and aging. In: Proceedings of the 25th Annual Meeting of the American Society of Biomechanics, San Diego. p 215–216.

Skedros JG, Dayton MR, Bachus KN. 2001b. Strain-mode specific loading of cortical bone reveals an important role for collagen fiber orientation in energy absorption. Trans Orthopaed Res Soc 26:519.

Skedros JG, Dayton MR, Sybrowsky CL, Bloebaum RD, Bachus NK. 2003a. Are uniform regional safety factors an objective of adaptive modeling/remodeling in compact bone? J Exp Biol 206:2431–2439.

Skedros JG, Sybrowsky CL, Dayton MR, Bloebaum RD, Bachus KN. 2003b. The role of osteocyte lacuna population density on the mechanical properties of cortical bone. Trans Orthopaed Res Soc 28: 414.

Skedros JG, Hunt KJ, Dayton MR, Bloebaum RD, Bachus KN. 2003c. The influence of collagen fiber orientation on mechanical properties of cortical bone of an artiodactyl calcaneus: implications for broad applications in bone adaptation. Trans Orthopaed Res Soc 28:411.

Steudel K. 1990a. The work and energetic cost of locomotion. I. The effects of limb mass distribution in quadrupeds. J Exp Biol 154: 273–285.

Steudel K. 1990b. The work and energetic cost of locomotion. II. Partitioning the cost of internal and external work within a species. J Exp Biol 154:287–303.

Stover SM, Pool RR, Martin RB, Morgan JP. 1992. Histologic features of the dorsal cortex of the third metacarpal bone mid-diaphysis during postnatal growth in thoroughbred horses. J Anat 181:455–469.

Swartz SM. 1990. Curvature of the forelimb bones of anthropoid primates: overall allometric patterns and specializations in suspensory species. Am J Phys Anthropol 83:477–498.

Swartz SM. 1993. Biomechanics of primate limbs. In: Gebo DL, editor. Postcranial adaptation in nonhuman primates. Dekalb: Northern Illinois University Press. p 5–42.

Taylor CR, Schmidt-Nielsen K, Raab JL. 1970. Scaling of energetic cost of running to body size in mammals. Am J Physiol 219:1104–1107.

Taylor CR, Heglund NC, Maloiy GMO. 1982. Energetics and mechanics of terrestrial locomotion. I. Metabolic energy consumption as a function of speed and body size in birds and mammals. J Exp Biol 97:1–21.

Taylor D. 1997. Bone maintenance and remodeling: a control system based on fatigue damage. J Orthop Res 15:601–606.
Taylor D, Lee TC. 1998. Measuring the shape and size of microcracks in bone. J Biomech 31:1177–1180.
van der Meulen MCH, Ashford Jr MW, Kiratli BJ, Bachrach LK, Carter DR. 1996. Determinants of femoral geometry and structure during adolescent growth. J Orthop Res 14:22–29.
Vaughan LC, Mason BJE. 1975. A clinico-pathological study of racing accidents in horses. Dorking: Bartholomew Press. 88 p.
Vose GP, Kubala ALJ. 1959. Bone strength: its relationship to x-ray determined ash content. Hum Biol 31:261–270.
Walker Jr WF, Liem KF. 1994. Functional anatomy of the vertebrates: an evolutionary perspective. 2nd ed. Fort Worth: Saunders College Publishing. 788 p.
Woo SL-Y, Keui SC, Amiel D, Gomez MA, Hayes WC, White FC, Akeson WH. 1981. The effect of prolonged physical training on the properties of long bone: a study of Wolff's law. J Bone Joint Surg 63-A:780–787.
Wright TM, Hayes WC. 1976. Tensile testing of bone over a wide range of strain rates: effects of strain rate, microstructure and density. Med Biol Eng 14:671–680.
Yeni YN, Brown CU, Wang Z, Norman TL. 1997. The influence of bone morphology on fracture toughness of the human femur and tibia. Bone 21:453–459.
Yeni YN, Norman TL. 2000. Calculation of porosity and osteonal cement line effects on the effective fracture toughness of cortical bone in longitudinal crack growth. J Biomed Mater Res 51:504–509.